POLITECNICO DI TORINO
Repository ISTITUZIONALE

Dispersion and mixing in quasigeostrophic turbulence

Original
Dispersion and mixing in quasigeostrophic turbulence / Bracco, A; von Hardenberg, J; Provenzale, A; Weiss, Jb; Mcwilliams, Jc. - In: PHYSICAL REVIEW LETTERS. - ISSN 0031-9007. - 92:8(2004). [10.1103/PhysRevLett.92.084501]

Availability:
This version is available at: 11583/2815020 since: 2020-04-22T14:18:45Z

Publisher:
AMERICAN PHYSICAL SOC

Published
DOI:10.1103/PhysRevLett.92.084501

Terms of use:

This article is made available under terms and conditions as specified in the corresponding bibliographic description in the repository

Publisher copyright

(Article begins on next page)

18 May 2024

Dispersion and Mixing in Quasigeostrophic Turbulence

Annalisa Bracco,[1] Jost von Hardenberg,[2] Antonello Provenzale,[2] Jeffrey B. Weiss,[3] and Jim C. McWilliams[4]
[1]*The Abdus Salam ICTP, I-34100 Trieste, Italy*
[2]*CIMA, Università di Genova, Genova, Italy and ISAC-CNR, Torino, Italy*
[3]*PAOS, University of Colorado, Boulder, Colorado 80309, USA*
[4]*Institute of Geophysics and Planetary Physics, UCLA, Los Angeles, California 90095-1567, USA*
(Received 15 August 2003; published 25 February 2004)

The dynamics of passive Lagrangian tracers in three-dimensional quasigeostrophic turbulence is studied numerically and compared with the behavior of two-dimensional barotropic turbulence. Despite the different Eulerian properties of the two flows, the Lagrangian dynamics of passively advected tracers in three-dimensional quasigeostrophic turbulence is very similar to that of barotropic turbulence. In both systems, coherent vortices play a major role in determining the mixing and dispersion properties. This work indicates that recent results on particle dynamics in barotropic, two-dimensional turbulence carry over to more realistic baroclinic flows, such as those encountered in the large-scale dynamics of the atmosphere and ocean.

DOI: 10.1103/PhysRevLett.92.084501 PACS numbers: 47.27.Eq, 47.27.Jv, 47.32.Cc, 92.10.Lq

The planetary-scale dynamics of the atmosphere and ocean is dominated by the rotation of the Earth and by strong, stable stratification. As a result, the vertical velocity is significantly smaller than the horizontal, and the large-scale motion is approximately two dimensional [1]. A simple model of this flow is a single layer of homogeneous fluid, described by the two-dimensional (2D) barotropic Navier-Stokes equations [2,3].

A barotropic model, however, lacks important aspects of the dynamics of geophysical flows, notably, the presence of baroclinic instability. A more realistic model is three-dimensional, baroclinic, quasigeostrophic (QG) turbulence, which still has zero vertical velocity but includes the vertical extent of the fluid. Several studies have focused on the Eulerian evolution of QG turbulence [4–7], but an analysis of its Lagrangian properties is still missing. A crucial question is whether the Lagrangian properties found in barotropic 2D flows still hold in baroclinic QG turbulence. In this Letter we study the dispersion and mixing behavior of Lagrangian tracers in uniformly stratified QG flows and compare with the 2D case.

We study the dynamics of freely decaying turbulence on the f plane, where the Coriolis parameter f is constant. 2D and QG have the same advection equation,

$$\frac{Dq}{Dt} = \frac{\partial q}{\partial t} + J[\psi, q] = \mathcal{D}, \tag{1}$$

where ψ is the stream function, $J[\psi, q] = \frac{\partial \psi}{\partial x}\frac{\partial q}{\partial y} - \frac{\partial \psi}{\partial y}\frac{\partial q}{\partial x}$ is the 2D horizontal Jacobian operator, and $\mathcal{D}$ is a generic dissipation term representing eddy viscosity. In QG flows, q is the 3D potential vorticity,

$$q = q_{3D} = \omega + \frac{\partial}{\partial z}\frac{1}{S(z)}\frac{\partial \psi}{\partial z}, \tag{2}$$

where the first term, $\omega = \nabla^2_{2D}\psi$, is the relative vorticity defined in terms of the 2D horizontal Laplacian, and the second term is the contribution of vortex stretching, with $S = N^2/f^2$, where N is the buoyancy frequency of the mean density stratification. Here we consider a uniformly stratified flow, and we assume constant S. In these conditions the coordinate transformation $z \to \sqrt{S}z$ reduces the operator in Eq. (2) to the isotropic three-dimensional Laplacian, ∇^2_{3D}. In 2D flow, q is the relative vorticity, $q_{2D} = \omega$.

In the absence of dissipative processes, both systems conserve the total energy, $E_\alpha = \frac{1}{2V_\alpha}\int d\mathbf{x}_\alpha |\nabla_\alpha \psi|^2$, and the enstrophy, $Z_\alpha = \frac{1}{V_\alpha}\int d\mathbf{x}_\alpha q_\alpha^2$, where, for $\alpha =$ 2D or 3D, V_α is the area or volume of the domain and $\mathbf{x}_\alpha$ is a two- or three-dimensional position vector, respectively. These conservation laws imply a preferential transfer of energy towards larger scales, an inverse cascade, and of enstrophy towards smaller scales, a direct cascade. For finite viscosity, both the energy and the enstrophy are dissipated. In the limit of vanishing viscous dissipation, however, these transfers lead to conservation of total energy and finite enstrophy dissipation. This differs from three-dimensional homogeneous isotropic turbulence where enstrophy is not conserved for zero viscosity and energy is not conserved for vanishing viscosity. To allow for a quantitative comparison between QG and 2D flows, we adopted a purely horizontal diffusion operator $D = (-1)^{n+1}\nu_p \nabla^{2n}_{2D} q$. It has been shown ([8] among others) that at high resolution, the use of hyperviscosity ($n > 1$) does not affect the statistical properties of the flow on scales larger than the dissipative range. In the following, we set $n = 2$ and $\nu_2 = 10^{-8}$. Similarly, changing the dissipation operator from horizontal to isotropic has a modest effect on the spectrum shape and causes no qualitative changes in the Eulerian evolution [4,5].

 © 2004 The American Physical Society

The QG and 2D equations are numerically integrated on a periodic domain, using the finite-difference algorithm described in [9], with a horizontal resolution of 512^2 grid points and, for QG, 256 grid points in the vertical. In both flows, passive Lagrangian tracers are advected by the horizontal Eulerian velocity.

The QG flow is initialized with a zero mean, Gaussian vorticity field with random Fourier phases. The initial energy spectrum is given by $E(k) = C_0 k^\beta/(k^{2\beta} + k_0^{2\beta})$, with $\beta = 10$ and $k_0 = 22$, and C_0 such that $\int E(k)dk = 1$. During the initial evolution the flow self-organizes into a collection of coherent vortices [4,5]. A three member ensemble of 2D flows is initialized by using horizontal sections of the QG stream function at time $t = 5$, past the vortex formation period. Such initialization guarantees identical kinetic energies, eddy-turnover time, Reynolds number (Re), and relative vorticity field at $t = 5$ for QG and 2D. At the same time, 256^2 Lagrangian tracers are randomly deployed on these three levels in QG and in the three 2D simulations, and their positions are integrated forward in time. The number of particles is large enough to ensure convergence in the Lagrangian statistics considered. Eulerian velocities are interpolated at the particle positions by using a local cubic interpolator. Using the same initial stream functions highlights the different evolution of QG and 2D flows. Indeed, the simulations presented are explicitly constructed to have the maximum similarity between QG and 2D at the deployment of the tracers. In the course of time, the Eulerian statistical properties of the QG and 2D flows gradually diverge and the difference between the systems grows as they evolve away from their initial conditions.

We first focus on the Eulerian characteristics of the flows. After $t = 5$, the vortex population evolves through mutual vortex advection and strong intermittent, inelastic interaction of same-sign vortices [4–6]. Figure 1 shows a 3D visualization of potential vorticity q_{3D} at $t = 20$. Despite the mathematical and dynamical analogies between 2D and QG flows, there are quantitative differences in the stability properties of vortices and filaments [7,10], in the merging mechanism [7], and in the decay rate of the vortices [5]. The faster decay of the vortex number in the QG flow is reflected by a faster enstrophy decay. The total energy, on the other hand, is nearly conserved in both systems. Figure 2 shows horizontal sections of the relative vorticity field, at times $t = 5$, when ω is the same for 2D and QG, and at time $t = 20$, when the difference in vortex number is evident. At late times, the background of the QG solution is populated by a larger number of filaments which carry a significant amount of vorticity and are bounded by curves of local maxima of (potential) vorticity gradient. In the 2D case, the background between the vortices is characterized by a low, more uniformly distributed vorticity content. Because of the higher probability of inelastic interactions in QG, filaments are produced at a higher rate. Analyzing their signature in the vorticity gradient field, we find that they live longer than their 2D counterparts. In 2D, filaments are rapidly reduced through stretching and dissipation, while in QG some individual filaments can be tracked from $t = 5$ to the end of the integration. Figure 3 shows the evolution of the one-point probability density function (PDF) of the relative vorticity field, averaged over the three selected levels in QG and over the three realizations in 2D. In the 2D case, the tail of the PDF exhibits little decay, while the central core of the distribution narrows significantly with time [11,12]. In the QG case, the tail of the PDF decays faster, consistent with the presence of fewer vortices, while the core is slightly broader, consistent with a larger number of filaments.

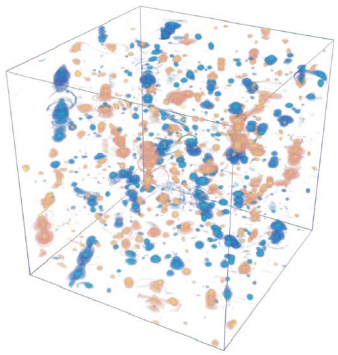

FIG. 1 (color online). q_{3D} with transparency rendering at $t = 20$.

The observation that 3D vorticity filaments in QG turbulence dissipate more slowly than their 2D counterparts indicates that QG dynamics is less efficient in transferring vorticity from the filaments to the dissipation scale. This transfer, which is related to filament stretching and shearing and is controlled by the large-scale strain field induced by the vortices, depends on the Reynolds number and on the range of the interactions [13]. In QG, the Green's function decreases as the inverse of distance, while in 2D it is logarithmic. Therefore, for flows at the same Re, QG vortices have a shorter range of interaction and they induce in the background strain and adverse shear which is weaker than that induced by their 2D counterparts. Thus, the shearing effect of the vortices on the filaments is weaker in QG than in 2D.

The Eulerian population of vortices and filaments determines the Lagrangian dispersion properties of the two flows. One measure of global dispersion is absolute (or single-particle) dispersion [14]. Absolute dispersion is defined as the average squared distance of the particle positions at time t from their initial positions at time t_0, $A^2(t; t_0) = \langle |\mathbf{x}(t) - \mathbf{x}(t_0)|^2 \rangle$. At sufficiently small times the absolute dispersion is ballistic, $A^2 = 2E\tau^2$, where E is the average kinetic energy and $\tau = t - t_0$. After a sufficiently long time, in statistically stationary flows with finite spatial correlation length, the velocities of

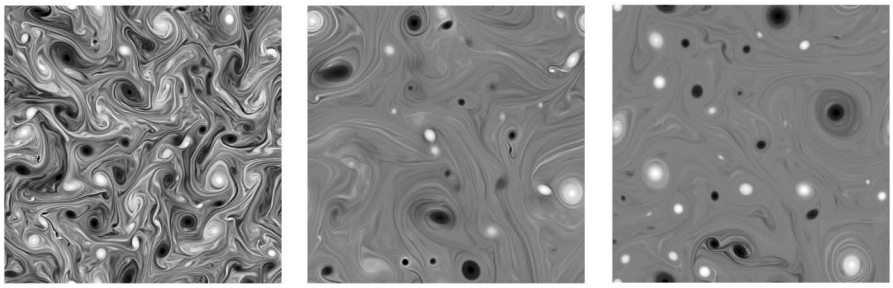

FIG. 2. Relative vorticity in a selected horizontal plane for the QG simulation at times (a) $t = 5$ and (b) $t = 20$. Panel (c) shows the relative vorticity field at $t = 20$ for a 2D simulation initialized with the vorticity distribution of panel (a).

the particles become uncorrelated and the dispersion is Brownian, $A^2 = 2K\tau$, where K is the (constant) dispersion coefficient. In freely decaying turbulence, the Brownian limit is not attained and the long-time limit depends on the details of the flow. Similarly, Brownian dispersion is rarely observed in mesoscale ocean flows, where large-scale spatial and temporal inhomogeneities prevent the presence of a well-defined Brownian regime. Rather, in geophysical flows one is often interested in the behavior of particle dispersion at intermediate times. In 2D turbulent flows, where vortices occupy a relatively small area, absolute dispersion is dominated by particles moving in the background turbulence outside the vortices and an anomalous intermediate-time regime $A^2 \propto \tau^{5/4}$ appears [15]. When scaled to midocean conditions, this regime is observed to hold for times ranging from a few days to a few weeks, which is a time range of practical interest. Indications of this anomalous dispersion regime have been detected in the analysis of subsurface ocean floats [16]. Figure 4 shows the absolute dispersion for particles moving in QG and 2D, obtained by averaging over all particles deployed at the three levels in QG and in the three corresponding 2D solutions. Because of the initial conditions, the ballistic dispersion regime is constrained to be identical for both systems. Surprisingly, however, the similarity continues at larger times, well past the ballistic regime. Indeed, absolute dispersion in QG is almost identical to that in 2D, with both displaying clear evidence of the anomalous dispersion regime with $A^2 \propto \tau^{5/4}$.

Another measure of particles behavior is relative dispersion, which describes the average separation of particle pairs, $R(\tau)^2 = \langle |\mathbf{x} - \mathbf{x}'|^2 \rangle$, where $\mathbf{x}$ and $\mathbf{x}'$ are the positions of two (initially nearby) particles computed at the same time. For 2D turbulence, classical dispersion ideas predict $R^2 \propto \tau^3$ when the separation is in the energy cascade range [17] and exponential growth in the enstrophy cascade range [18]. Numerical simulations and experiments [19] confirm the presence of the τ^3 law, while the exponential regime reduces to a short transient stage. We calculate $R^2(\tau)$ for both QG and 2D by adding a companion to each particle at $t_0 = 5$, with a separation of one-quarter of the grid spacing randomly oriented in space. Figure 4 shows the relative dispersion curves for QG and 2D. Both QG and 2D show an intermediate Richardson regime and display no substantial differences.

Another important Lagrangian property is mixing. One quantitative measure of mixing commonly used in 2D turbulence is the maximum Lagrangian finite-time Lyapunov exponent (FTLE), λ, which gives a local description of the stretching experienced by a fluid particle

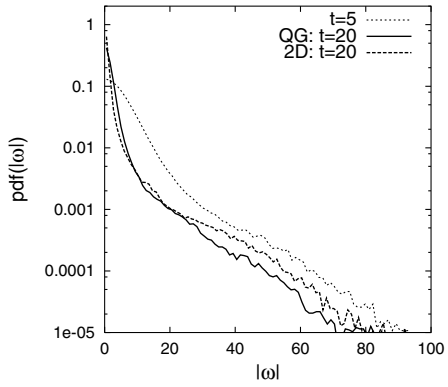

FIG. 3. Vorticity PDF at times $t = 5$ (dotted line), and $t = 20$ for the QG (solid line) and 2D (dashed line) cases, averaged over three horizontal planes in QG, and over the three 2D solutions.

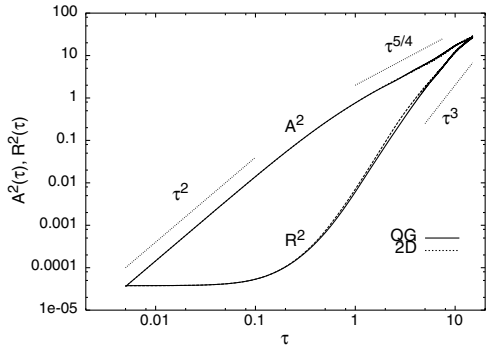

FIG. 4. Absolute dispersion, A^2, and relative dispersion, R^2, vs the time interval $\tau = t - t_0$, with $t_0 = 5$. Solid lines refer to QG and dashed lines to 2D. Dotted lines show the Richardson prediction for relative dispersion, $R^2 \propto \tau^3$, and the ballistic regime, $A^2 \propto \tau$, and the intermediate anomalous regime, $A^2 \propto \tau^{5/4}$, for absolute dispersion.

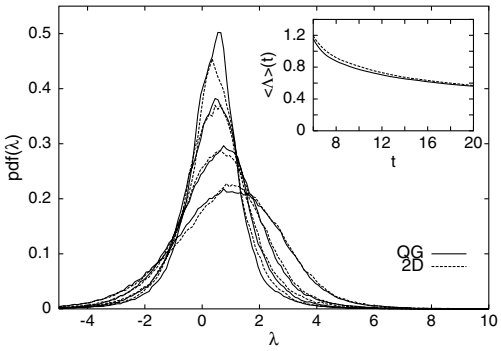

FIG. 5. Probability distribution functions of the FTLE, λ, for the set of Lagrangian particles advected on three horizontal planes of the QG simulation (solid lines) and in the corresponding 2D simulations (dashed lines). The FTLE have been computed over the finite time $T_\lambda = 0.25$ starting at $t = 6$, 10, 15, and 19.75. The inset shows the evolution of the time integral of the mean value of the FTLE, $\langle\Lambda\rangle(t)$, as a function of time.

[20]. Large values of λ correspond to regions of high strain which usually surround the vortices, while small values correspond to either vortex cores or regions of the background that are sufficiently far from the vortices or filaments. Figure 5 shows the values of λ, computed over the short finite time $T_\lambda = 0.25$, for all the particles deployed in the three levels in QG and in the three 2D solutions. Overall, the mixing properties, as measured by the distribution of the FTLE's, are nearly the same. The PDF's of λ evolve similarly up to time $t = 15$. Later on the 2D case displays a slight excess of large positive FTLE's and a deficit of small positive FTLE's with respect to the QG case, consistent with the growing differences between QG and 2D in the vortex number and in filament populations.

This time approximately marks the end of the intermediate regime where the Lagrangian properties are the same in QG and 2D. The inset in Fig. 5 shows the mean value of the time-integrated FTLE, $\langle\Lambda\rangle = 1/t \int\langle\lambda\rangle dt$, which is very similar for the two flows.

In summary, uniformly stratified QG turbulence and barotropic 2D turbulence display an extremely similar Lagrangian dynamics at short and intermediate times. Since we analyzed only one realization of the QG flow and a few realizations of 2D flows, we cannot exclude that other initial conditions could lead to different results. However, since 2D turbulence has limited predictability, there should be no significant dependence on the initial conditions beyond the Lagrangian velocity decorrelation time. Our results therefore indicate that, for both QG and 2D, the Lagrangian dynamics is governed by the coherent vortices in a similar way, and the three dimensionality of QG vortices does not play a relevant role in Lagrangian dispersion. Although the initial conditions were chosen to be the same for 2D and QG, the long-time evolution of the two flows diverges, and so does the Lagrangian dynamics. On intermediate times, however, the Lagrangian dynamics of QG and 2D remain extremely similar, and the behavior previously detected in Lagrangian studies of barotropic turbulence is also seen in more realistic 3D QG flows. The local mixing properties, as measured by finite-time Lyapunov exponents, are comparable, and the absolute and relative dispersions are nearly identical. When scaled to midocean conditions, this correspondence holds for dispersion times up to several weeks.

This work thus suggests that recent results on the dispersion and mixing properties of barotropic, vortex dominated flows are also relevant for understanding Lagrangian processes in baroclinic geophysical turbulence at a low Rossby number in the atmosphere and ocean.

The authors acknowledge support from CINECA, Bologna, Italy. A. B. was partially supported by W.H.O.I., and J. B. W. was partially supported by NSF OCE-9818839.

[1] J. Charney, J. Atmos. Sci. **28**, 1087 (1971).
[2] J. C. McWilliams, J. Fluid Mech. **146**, 21 (1984).
[3] A. Provenzale, Annu. Rev. Fluid Mech. **31**, 55 (1999).
[4] J. C. McWilliams, J. B. Weiss, and I. Yavneh, Science **264**, 410 (1994).
[5] J. C. McWilliams, J. B. Weiss, and I. Yavneh, J. Fluid Mech. **401**, 1 (1999).
[6] D. G. Dritschel, M. de la Torre Juàrez, and M. H. P. Ambaum, Phys. Fluids **11**, 1512 (1999).
[7] J. von Hardenberg *et al.*, J. Fluid Mech. **412**, 331 (2000).
[8] I. Yavneh and J. C. McWilliams, J. Sci. Comput. **11**, 47 (1996).
[9] A. Shchepetkin and J. C. McWilliams, Mon. Weather Rev. **126**, 1541 (1998).
[10] D. W. Waugh and D. G. Dritschel, J. Atmos. Sci. **56**, 2359 (1999).
[11] P. Bertello and T. Warn, J. Fluid Mech. **326**, 357 (1996).
[12] A. Bracco *et al.*, Phys. Fluids **12**, 2931 (2000).
[13] P. Protas, A. Babiano, and N.-R. Kevlahan, Physica (Amsterdam) **128D**, 169 (1999).
[14] A. Monin and A. M. Yaglom, *Statistical Fluid Mechanics* (MIT Press, Cambridge, 1971).
[15] D. Elhmaïdi, A. Provenzale, and A. Babiano, J. Fluid Mech. **257**, 533 (1993).
[16] V. Rupolo, B. L. Hua, A. Provenzale, and V. Artale, J. Phys. Oceanogr. **26**, 1591 (1996).
[17] L. F. Richardson, Proc. R. Soc. London A **110**, 709 (1926).
[18] R. H. Kraichnan, Phys. Fluids **9**, 1937 (1966).
[19] A. Babiano, C. Basdevant, P. L. Roy, and R. Sadourny, J. Fluid Mech. **214**, 535 (1990).
[20] A. Babiano, G. Boffetta, A. Provenzale, and A. Vulpiani, Phys. Fluids **6**, 2465 (1994).